Expression of Group IA Phospholipase A_2 in *Pichia pastoris*: Identification of a Phosphatidylcholine Activator Site Using Site-Directed Mutagenesis†

Lee J. Lefkowitz, Raymond A. Deems, and Edward A. Dennis*

Department of Chemistry and Biochemistry, University of California, San Diego, La Jolla, California 92093-0601

Received June 22, 1999; Revised Manuscript Received August 16, 1999

ABSTRACT: Site-directed mutants of the group IA phospholipase A_2 from cobra venom were constructed and expressed in the methylotrophic yeast *Pichia pastoris* to probe for the proposed phosphatidylcholine (PC) activator site. Previous crystallographic and molecular modeling studies have identified two regions of the enzyme as likely candidates for this site. Residues Glu-55, Trp-61, Tyr-63, Phe-64, and Lys-65 were mutated to test the site advanced by Ortiz et al. [(1992) *Biochemistry 31*, 2887−2896] while Asp-23 and Arg-30 were mutated to assess the site proposed by Segelke et al. [(1998) *J. Mol. Biol. 279*, 223−232]. Expressed enzymes were purified by affinity chromatography and analyzed by SDS−PAGE, Western blotting, electrospray ionization mass spectroscopy, and circular dichroism. Both phospholipid headgroup specificity and rates of hydrolysis on monomeric PC substrates were determined and found to be similar for native, wild-type, and all of the mutant enzymes. These results suggest that all of the expressed enzymes were properly folded and contained functional catalytic sites. Mutations of the aromatic residues in the Ortiz site generally had little effect on PC activation, arguing against the importance of this region of the enzyme for PC activation; however, these aromatic amino acids appeared to be important for interfacial activation. In contrast, the D23N mutant in the Segelke site reduced PC activation by 10-fold without affecting activity toward micellar phosphatidylethanolamine substrates. Similar results were found with the D23N/R30M double mutant, suggesting that this region is critical for PC activation. These results provide evidence for the Segelke site as a PC activator site that is distinct from the catalytic site.

Phospholipase A_2s (PLA_2)[1] comprise a superfamily of lipolytic enzymes that catalyze the hydrolysis of *sn*-glycerophospholipids to form lysophospholipids and free fatty acids (*1*−*3*). The most extensively studied phospholipases are the secretory group I, II, and III enzymes that are found abundantly in pancreatic tissues and the venoms of snakes, bees, and lizards. These secreted PLA_2s are characterized by their low molecular mass (12−16 kDa), millimolar calcium requirement, and six to eight disulfide bonds.

A unique kinetic property of PLA_2s from elapidae snakes, such as the Indian cobra *Naja naja naja*, is PC activation in which the hydrolysis of phosphatidylethanolamine (PE) is increased 10−20-fold in the presence of phosphocholine-(PC-) containing lipids (*4*−*6*). Several other PC-containing lipids including sphingomyelin, lyso-PC, dodecylphosphocholine, and dibutyryl-PC are also known to cause PC activation (*7*). The stereochemistry of the activator molecule does not appear to be critical since activation was observed with β-dipalmitoylphosphatidylcholine and D-dipalmitoylphosphatidylcholine (*6*). Additionally, several synthetic thio-PC phospholipid analogues also display PC activation (*8*). Together, these findings highlight the requirement for the presence of the phosphocholine moiety for PC activation, although *N*,*N*-dimethylphosphatidylethanolamine also leads to modest activation (*6, 9*). While phosphatidylcholine, lyso-PC, sphingomyelin, and dodecylphosphocholine are all good activators, phosphocholine and glycerophosphocholine have no effect on activation, emphasizing the importance of at least one fatty acyl or alkyl chain for PC activation. PC activation is not observed with short-chain monomeric substrates. Rates of hydrolysis on monomeric substrates are nearly 100-fold lower than those of short-chain micellar substrates, but both short-chain PE and PC substrates are hydrolyzed at comparable rates. These findings demonstrate that an interface is required to observe PC activation (*10, 11*). Therefore, the minimal requirements for PC activation include a phosphocholine headgroup, at least one fatty acyl or alkyl chain, and an interface (*6, 7, 12*).

These observations led to the postulation of a two-site model: an activator site with PC specificity and a separate catalytic site with a preference for zwitterionic phospholipids (*12*−*14*). Recently, experimental evidence for the existence of such a noncatalytic PC binding site was provided by equilibrium dialysis experiments showing that a monomer of *N. naja naja* PLA_2 contains two sites that bind a nonhydrolyzable PC analogue (S. C. Boegeman and E. A. Dennis, manuscript in preparation).

† This work was supported by a grant from the National Institutes of Health, GM 20501. L.J.L. was the recipient of NIH predoctoral training grant 5 T32 DK07202. The authors acknowledge the kind gift of a New Brunswick BioFlow 3000 Fermentor from Central Soya, Inc.

* To whom correspondence should be addressed. Telephone: 858-534-3055. Fax: 858-534-7390. E-mail: edennis@ucsd.edu.

[1] Abbreviations: diC_6-PC, 1,2-dihexanoyl-*sn*-glycero-3-phosphocholine; endo Arg-C, endoproteinase Arg-C; PC, phosphatidylcholine; PE, phosphatidylethanolamine; PLA_2, phospholipase A_2; PLPC, 1-palmitoyl-2-linoleoyl-*sn*-glycero-3-phosphocholine; PLPE, 1-palmitoyl-2-linoleoyl-*sn*-glycero-3-phosphoethanolamine; TLC, thin-layer chromatography; Tris, tris(hydroxymethyl)aminomethane; TX-100, Triton X-100; WT, wild type.

10.1021/bi991432t CCC: $18.00
Published on Web 10/07/1999

Two regions of the cobra PLA_2 have been identified as possible sites for the second PC binding site. The first suggestion was advanced by Ortiz et al. (*15*). Their modeled structure of *Naja naja kaouthia* PLA_2 reveals a possible binding site with good steric and electrostatic complementarity to phosphocholine that is located near the elapid loop. This site is approximately 80% similar to a region of the McPC603 antibody that recognizes phosphocholine. Residues important for PC recognition include[2] Glu-55, Trp-61, Tyr-63, Phe-64, and Lys-65. A second site advanced by our laboratory suggests that the noncatalytic PC binding site may be located near Asp-23 and Arg-30 (*16*). As these two hypotheses have not been tested experimentally, we have now employed site-directed mutagenesis to determine which of these residues affect PC activation.

MATERIALS AND METHODS

Reagents. Phospholipids were purchased from Avanti Polar Lipids, Inc. (Alabaster, AL). Affi-Gel Blue resin was from Bio-Rad. DE23 resin was from Whatman BioSystems Ltd. (Kent, England). *Pichia pastoris* strains and vectors were obtained from Invitrogen (Carlsbad, CA). Oligonucleotide primers were purchased from either Genosys (Woodlands, TX) or Gibco BRL (Bethesda, MD). Endoproteinase Arg-C was from Boehringer Mannheim (Cleveland, OH). Radiolabeled phospholipids, restriction enzymes, and DNA modifying enzymes were from Amersham Pharmacia Biotech (Piscataway, NJ). Mutagenesis was carried out with the QuickChange Mutagenesis kit from Stratagene (La Jolla, CA). All other chemicals were of at least analytical grade and were obtained from either Fisher or Sigma.

Cloning. The gene encoding *N. naja naja* PLA_2 was transferred from the *Escherichia coli* expression vector pRC25/Xa/NNNPLA_2 (*17, 18*) to the *P. pastoris* expression vector pPIC9K*Nnn*PLA_2. This construct served as template DNA for Stratagene's Quick Change PCR-based mutagenesis system. Due to the large size of the pPIC9K*Nnn*PLA_2 vector (9.6 kb), it was sometimes easier to first subclone the PLA_2 gene into the smaller pUC19 vector before carrying out PCR. This step was carried out by digesting the pPIC9K*Nnn*PLA_2 vector with *Sac*I−*Sal*I and subcloning the PLA_2 gene fragment into the *Sac*I−*Sal*I linearized pUC19 vector. The resultant pUC19PLA_2 vector was then used in subsequent PCR mutagenesis steps. Following PCR, the mutated PLA_2 gene was transferred back to the pPIC9K*Nnn*PLA_2 vector for transformation into yeast.

Mutagenesis. Site-directed mutants were constructed using the Stratagene Quick Change PCR-based mutagenesis system according to the manufacturer's instructions. Coding and noncoding mutagenic primers were used to PCR amplify either the entire pPIC9K*Nnn*PLA_2 or pUC19PLA_2 vector with *Pfu* polymerase (a list of primers used can be obtained from the authors). Removal of the methylated template DNA was accomplished by digestion with *Dpn*I, a restriction enzyme that cleaves only methylated DNA. Since mutant DNA produced by PCR amplification is unmethylated, it was not digested by *Dpn*I and could be used directly to transform XL-2 Blue Ultracompetent cells. Colonies growing on LBA plates were screened by restriction enzyme digest analysis. Positive colonies were confirmed by sequencing the entire PLA_2 gene using either manual sequencing based on the method of Sanger (*19*) or via an Applied Biosystems automated DNA sequencer.

Transformation and Selection. The protease-deficient *P. pastoris* strain SMD1168 was transformed using 10 μg of the *Bgl*II fragment of pPIC9K*Nnn*PLA_2 that contained the gene of interest using a spheroplasting method described previously (*20, 21*). All media and plates for *P. pastoris* gene expression were made according to the manufacturer's recommendations. Transformants growing on histidine-deficient RDB plates (4.5% potassium chloride, 2% glucose, 1% ammonium sulfate, 0.34% yeast nitrogen base, and 0.05% biotin) were pooled and plated on MD plates (1% ammonium sulfate, 2% glucose, 0.34% yeast nitrogen base, and 0.05% biotin) to yield 200−400 colonies per plate. Selection of high copy number transformants was accomplished by replica plating to YPD plates (1% yeast extract, 2% peptone, and 2% glucose) containing 2 g/L antibiotic G418. Typically 10 colonies would grow on the G418 plates, and these were screened for PLA_2 activity. Individual colonies were selected and used to inoculate 10 mL of BMGY media (1% yeast nitrogen base, 1% glycerol, 1% casamino acids, and 0.05% biotin) and allowed to grow with shaking for 2 days at 30 °C. Cells were pelleted by centrifugation at 3000*g* for 3 min, and the media were discarded. Induction was begun by resuspending the cells in 5 mL of BMMY media (identical to BMGY media except that 1% methanol was substituted for glycerol) and grown with shaking at 30 °C for 2 days. After 1 day of induction, the media were supplemented with 1% methanol. Following 2 days of methanol induction, a sample of media was taken and centrifuged at 12 000 rpm in an Eppendorf microfuge to pellet the cells. A 7 μL aliquot of this cell-free media was then assayed using the spectrophotometric assay described below. Samples with the highest activity were chosen for high-level expression using either shake flasks or a New Brunswick fermentor.

Expression. Selected colonies of D23N, R30M, D23N/R30M, E55Q, Y63A, Y63F, K65M, and W61A/Y63A/F64A were expressed in 4 L baffled shake flasks. Several microliters of a frozen stock was used to inoculate a 10 mL overnight culture of BMGY. The next morning this seed culture was used to inoculate 1 L of BMGY in a 4 L baffled shake flask and allowed to grow with shaking for 2 days at 30 °C. The media were next centrifuged at 3000*g* for 10 min at 4 °C to pellet the cells. The BMGY media were discarded, and the cells were resuspended in 200 mL of BMMY to begin induction. After being transferred to a different 4 L baffled flask, the cells were allowed to grow for 2 days with shaking at 30 °C. Following 1 day of induction, methanol was added to 1% (v/v) to compensate for loss due to evaporation. After 48 h of methanol induction, the cell suspension was centrifuged at 3000*g* for 10 min at 4 °C to pellet the cells. Cells were discarded, and the crude media were stored frozen at −20 °C.

The highest producing strains of WT, W61A, and F64A were expressed in a 5.0 L BioFlow 3000 fermentor (New Brunswick Scientific) essentially as described previously (*22*). Seed cultures were generated by inoculating 10 mL of

[2] *N. naja naja and N. naja kaouthia* PLA_2 are numbered consecutively according to their primary sequence. These enzymes differ at only 6 out of 119 amino acids, and none of these differences are located in the PC activator site proposed by Ortiz et al. (*15*).

BMGY with 10−20 μL of cells from a glycerol stock. After 24 h this culture was used to inoculate 250 mL of BMGY and allowed to grow with shaking at 30 °C overnight. This seed culture was next added to 3.0 L of Basal salts media (1.3 mL/L 85% phosphoric acid, 1.8 g/L calcium sulfate, 14.3 g/L potassium sulfate, 11.7 g/L magnesium sulfate heptahydrate, 3.9 g/L potassium hydroxide, 40 g/L glycerol, and 4 mL/L PTM4 salts). PTM4 salts consisted of 2 g/L cupric sulfate pentahydrate, 0.08 g/L sodium iodide, 3 g/L manganese sulfate, 0.2 g/L sodium molybdate dihydrate, 0.02 g/L boric acid, 0.5 g/L cobalt chloride, 7 g/L zinc chloride, 0.2 g/L biotin, 22 g/L ferrous sulfate heptahydrate, and 1 mL/L sulfuric acid. After 24 h of the Glycerol Batch Phase, the cell density increased to a wet cell weight of approximately 130 mg/mL. At this stage, a Fed-Batch Glycerol Phase was begun by feeding in a 1.0 L solution of 50% glycerol plus 12 mL/L PTM4 salts ramped from 18 mL/h to 45 mL/h over 8 h and then left at 45 mL/h for an additional 16 h until the 1.0 L was depleted and the wet cell weight had increased to approximately 330 mg/mL. Prior to methanol induction, the glycerol feed was disconnected and the cells were allowed to deplete any glycerol remaining in the media for 30 min to 2 h. Induction was initiated by ramping the addition of a 50% methanol solution containing 6 mL/L PTM4 salts from 1.8 mL/h to 21.6 mL/h over 8 h. Cells were then switched to a 100% methanol solution containing 12 mL/L PTM4 salts and ramped from 10.8 mL/h to the maximum methanol feed rate tolerated by the yeast which was usually 18−25 mL/h depending on the strain. Activity was monitored using the spectrophotometric assay described below and typically peaked after 48 h of methanol induction. Runs were terminated at this time and purification was initiated.

Protein Purification. Following fermentation, crude media were centrifuged at 3000*g* to remove the cells. The crude media were then decanted into 1 L bottles and stored frozen at −20 °C. To begin the purification process, the crude media were thawed and centrifuged at 15000*g* to pellet any remaining cells and proteins that had aggregated during freezing. This step also reduced the viscosity of the crude media, enabling it to be directly applied to a 5 cm by 30 cm Affi-Gel Blue gravity flow column equilibrated with 50 mM ammonium acetate, pH 6.0, at a flow rate of 15 mL/min. After the column was loaded, 2 volumes of pH 6.0 buffer was used to wash the column until the A_{280} approached baseline. Two column volumes of 20 mM ammonium bicarbonate, pH 8.0, was then used to elute loosely bound proteins. Upon reaching baseline, PLA_2 was eluted using 20 mM ammonium carbonate, pH 10.5. The PLA_2 fraction was pooled and neutralized immediately with glacial acetic acid. This fraction was then dialyzed against three exchanges of milliQ water at 4 °C before being lyophilized. Following lyophilization, the protein powder was dissolved in a minimum volume (2−3 mL) of sterile water.

SDS−PAGE analysis of the enzymes expressed via fermentation revealed a doublet of 13−14 kDa with minor contaminants. N-Terminal sequencing of the PLA_2 band revealed that 60−80% of the protein was native PLA_2 but that 20−40% of the protein contained an arginine or lysine−arginine addition at the N-terminus presumably due to incorrect processing of the signal sequence in the *P. pastoris* secretion pathway. Mutants expressed in shake flasks did not have any N-terminal modifications and did not require further purification. To remove the N-terminal adjunct from enzymes produced using fermentation, digestion with endoproteinase Arg-C (endo Arg-C) was carried out. Endo Arg-C was dissolved in milliQ water to 100 units/mL. The reaction was carried out in 10 mM Tris, pH 7.5, 1 mM DTT, 10 mM $CaCl_2$, and 1.59 mM TX-100 at 30 °C overnight. One unit of endo Arg-C was used per 58 μg of PLA_2. The endo Arg-C was removed via ion-exchange chromatography with DE23 resin utilizing conditions identical to those described previously with DE11 resin (*23*) except that protein was loaded in 20 mM NaH_2PO_4, pH 6.0.

Protein Determination. Protein concentrations were determined by the method of Lowry (*24*) using the correction factor for *N. naja naja* PLA_2 described previously (*25*).

Enzyme Assays. PLA_2 activity was determined using several assays. A spectrophotometric assay (*18, 26*) was used to monitor enzyme activity during the induction of *P. pastoris* cultures. These assays were carried out at 30 °C and employed 0.5 mM *rac*-diC_{10}-dithio-PC, 2.26 mM TX-100, 10 mM $CaCl_2$, 25 mM Tris, pH 8.5, and 100 mM KCl. Assays were initiated by the addition of enzyme and 7 μL of 4,4′-dithiobispyridine to 0.4 mL of substrate. The free thiol liberated by PLA_2 hydrolysis was monitored by following the increase in absorbance at 324 nm.

The rates of hydrolysis of monomeric diC_6-PC were determined using a modification of a thin-layer chromatography (TLC) assay described previously (*4, 27, 28*). Briefly, reactions were run at 40 °C with 0.8 mM diC_6-PC, 25 mM Tris, pH 8.5, and 10 mM $CaCl_2$ in a final volume of 400 μL. Reactions were stopped by the addition of 400 μL of 5% HCl (v/v), and lipids were extracted with 400 μL of 1-butanol. The 1-butanol layer was dried under vacuum. Dried lipid was redissolved in 25 μL of chloroform/methanol (1:2) and spotted on TLC plates (20 × 20 cm Merck KGaA, Darmstadt, Germany) using chloroform/methanol/28% ammonium hydroxide (65:25:5) as the mobile phase. R_f values were 0.38 for phospholipid and 0.08 for lysophospholipid. The total phosphate concentration of the phospholipid zone was determined using a modification (*29*) of the procedure described by Bartlett (*30*). Specific activities were calculated on the basis of the rate of phospholipid conversion to lysophospholipid. Control experiments were performed to ensure that extraction efficiencies were uniform across the concentration ranges tested.

Measurements of phospholipid hydrolysis in the presence or absence of sphingomyelin were carried out using a modified Dole assay (*31*). Substrate was prepared by drying phospholipid stocks in chloroform under a stream of nitrogen. To accelerate the evaporation of solvent, the test tube containing phospholipid was routinely warmed to 37 °C in a water bath. Dried lipid was resuspended in an appropriate amount of TX-100 and diluted with buffer to a final concentration of 300 μM phospholipid, 2.4 mM TX-100, 25 mM Tris, pH 8.5, and 10 mM $CaCl_2$. Sufficient radiolabeled 1-palmitoyl-2-[1-^{14}C]linoleoyl-*sn*-glycero-3-phosphoethanolamine (PLPE) or 1-palmitoyl-2-[1-^{14}C]linoleoyl-*sn*-glycero-3-phosphocholine (PLPC) was included to provide approximately 100 000 cpm per assay. Reactions were initiated by adding 400 μL of substrate to 100 μL of enzyme and allowed to proceed for 15−45 min at 40 °C with agitation. To quench the reaction, 2.5 mL of Dole reagent [2-propanol/heptane/1

N H_2SO_4, 20:5:1 (v/v/v)] was added followed by about 0.1 g of silica gel, 1.5 mL of heptane, and 1.5 mL of deionized water. After vortexing and phase separation, 1 mL of the upper heptane layer was removed and passed through a column containing approximately 0.1 g of silica gel. Any remaining radiolabeled fatty acid was washed off the column with 1 mL of ether. An aliquot of the organic layer was added to 5 mL of scintillation fluid and counted in a Packard TR1600 liquid scintillation analyzer.

Western Blotting. Proteins were separated on 18% Tris−glycine gels (Novex) and transferred to Immobilon-P membranes (Millipore). Nonspecific binding was blocked by incubating membranes in 5% nonfat milk in phosphate-buffered saline (Sigma) for 1 h. An antibody against *N. naja naja* PLA_2 was diluted 1:500 in blocking buffer and incubated with the membrane for 1 h. Rabbit anti-goat immunoglobin conjugated to horseradish peroxidase (Dako) was used as the secondary antibody and facilitated detection by enhanced chemiluminesence (Amersham).

Circular Dichroism. CD spectra were recorded essentially as described previously using 0.1 cm quartz cuvettes (*32*). Samples contained approximately 0.4 mL of 0.15 mg/mL PLA_2 in 10 mM $CaCl_2$. Spectra were recorded on an AVIV spectropolarimeter. To convert millidegrees to mean residue ellipticity, values were multiplied by 100 × mean residue weight/(*cd*), where *c* is the protein concentration in milligrams per milliliter and *d* is the path length in centimeters.

RESULTS

Rationale for Mutations. A putative PC activator site for group IA PLA_2s was advanced by Ortiz et al. (*15*) on the basis of the results of molecular modeling studies. Stabilization of the positively charged choline headgroup is proposed to occur primarily via cation-π interactions (*33*) between the choline headgroup and the aromatic amino acid side chains of Trp-61, Tyr-63, and Phe-64. Minor stabilization of the choline headgroup could also be achieved by long-range electrostatic interactions with Glu-55. The negatively charged phosphate would also be in position to interact with Lys-65. To test this hypothesis, the aromatic amino acids at positions Trp-61, Tyr-63, and Phe-64 were mutated to alanine to disrupt any potential cation−π interactions. To analyze the contribution made by the hydroxyl group of the Tyr-63 side chain, the Y63F mutant was also constructed. Additionally, we constructed the W61A/Y63A/F64A triple mutant to remove all three aromatic amino acids. The roles of Glu-55 and Lys-65 in providing minor electrostatic stabilization were probed by making the uncharged but sterically conserved E55Q and K65M mutants. The residues that comprise the Ortiz site are shown in yellow in Figure 1 and occupy the same face of the enzyme as the opening to the active site. The hydrophobic fatty acyl chain(s) of the activator molecule are presumed to remain associated with the interface and may anchor the enzyme to the interface during catalysis. If these residues are important for PC activation, one would expect that these mutations would decrease PC activation. It is important to note that only $sPLA_2$s from the elapidae family contain the amino acids needed to make these contacts and only PLA_2s from the venom of elapid snakes have been shown to exhibit PC activation.

An alternative region of the enzyme that could serve as a PC activator site has also been identified by our laboratory on the basis of crystallographic studies (*16*). When calcium is bound in the calcium binding loop, a conformational change creates a pocket with good steric and electrostatic complementarity to a PC headgroup and exposes the side chains of Asp-23 and Arg-30. The positive charge of the choline headgroup could make favorable contacts with the carboxylate on the side chain of Asp-23, the amide nitrogen of Arg-30, and the carbonyl oxygens of Gly-25 and Cys-28. Additionally, the guanidinium group of Arg-30 could form a salt bridge with the negatively charged PC phosphate group. To test this proposal, the D23N, R30M, and D23N/R30M mutants were constructed to see what effect removing one or both of these charges would have on PC activation. The residues that comprise the Segelke site are shown in red in Figure 1. Since this model contains the cofactor calcium, a salt bridge is not formed between Asp-23 and Arg-30. The surface views shown in Figure 2 highlight the dramatic changes to the solvent-exposed surface of the enzyme that accompany the rearrangement of the Arg-30 side chain when calcium is bound. As with the Ortiz site, the Segelke site also occupies the same face of the enzyme as the opening to the active site, and the hydrophobic fatty acyl chain(s) of the activator molecule are thought to remain associated with the interface where they may anchor the enzyme to the interface during catalysis.

FIGURE 1: Location of the proposed PC activator site in group IA PLA_2. A ribbon diagram of *N. naja naja* PLA_2 is shown in cyan. Residues proposed by Ortiz et al. (*15*) to be part of the PC activator site are shown in yellow (Glu-55, Trp-61, Tyr-63, Phe-64, and Lys-65), and those proposed by Segelke et al. (*16*) are shown in red (Asp-23 and Arg-30). A green PE substrate analogue is bound in the active site on the basis of results obtained from transfer NOE experiments (*45*). The cofactor calcium ion is shown in gray, the catalytic histidine in cyan, and the N-terminus in blue. This figure was generated using InsightII from Molecular Simulations, Inc. (San Diego, CA).

Cloning and Mutagenesis. As the first step in these studies, we developed a system to produce recombinant cobra venom

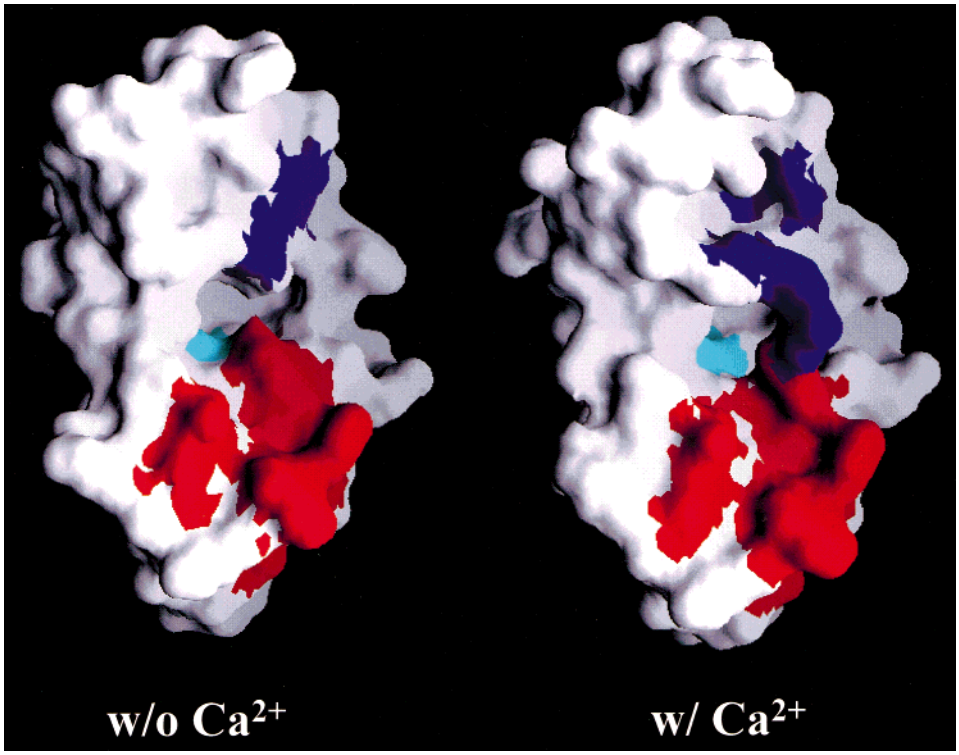

FIGURE 2: Rearrangements caused by calcium binding in the PC activator site. Surface views of the PC activator site proposed by Segelke et al. (*16*) are shown in blue while the site proposed by Ortiz et al. (*15*) is shown in red. The catalytic histidine is shown in cyan. Without the calcium cofactor bound, Asp-23 and Arg-30 form a salt bridge that is seen as a contiguous blue region. Upon calcium binding, a substantial rearrangement of Arg-30 occurs, opening up a pocket with good steric and electrostatic complementarity to a choline headgroup. Surface views were generated using GRASP (*46*).

PLA_2 in the methylotrophic yeast *P. pastoris*. Previous reports have demonstrated the suitability of this organism for expressing highly disulfide bonded proteins (*20*) with yields in the range of hundreds of milligrams per liter (*34*). The cloning steps used to generate the expression vector are shown in Figure 3. Amplification of the entire vector using *Pfu* polymerase and appropriate mutagenic primers yielded plasmids containing the various mutated versions of the PLA_2 gene. All mutations were confirmed by sequencing the entire PLA_2 gene.

Transformation of the mutant PLA_2 gene into the protease-deficient *P. pastoris* SMD1168 strain was carried out using a spheroplasting transformation procedure utilizing *Bgl*II-linearized pPIC9K*Nnn*PLA_2 (*20, 21*). Transformants containing multiple copies of the gene of interest were selected using plates containing G418, an analogue of kanamycin. Those strains containing the highest levels of PLA_2 activity were chosen for scaleup.

Protein Expression and Purification. Wild-type and mutant cobra PLA_2s were produced in *P. pastoris* using either shake flasks or a fermentor. Secretion into the growth media was directed by the α-factor secretion signal. Yields ranged from 400 μg/L to 2 mg/L for enzymes expressed in shake flasks and 5 mg/L to 30 mg/L for enzymes expressed using fermentation. Recombinant proteins were then purified using Affi-Gel Blue affinity chromatography as outlined in Materials and Methods. This single purification step was sufficient to produce homogeneous protein preparations of the enzymes that had been produced using shake flasks.

For enzymes expressed using the BioFlo 3000 fermentor, an additional purification step was required to produce pure protein since N-terminal sequencing demonstrated that approximately 20−40% of the enzyme contained a Lys−Arg or Arg adjunct on the N-terminus. This was presumably due to incomplete processing of the α-factor fusion protein by *P. pastoris* and proteolysis by an unidentified protease after the Asp or Lys residues that precede the KEX2 consensus sequence in the α-factor secretion signal. Due to concerns about the importance of the N-terminus for activity in other $sPLA_2$s (*35*), we elected to remove these residues with endo Arg-C (*36*). Regeneration of the expected N-terminus was confirmed by N-terminal sequencing (data not shown). Removal of the endo Arg-C was accomplished by ion-exchange chromatography using a DE-23 column. Fermentation usually produced a 10-fold better expression than shake flasks, but an equally important factor for obtaining high yields appeared to be selecting strains containing multiple gene inserts.

Following purification, native, WT, and mutant enzymes were loaded on 18% Tris−glycine gels and separated by SDS−PAGE under denaturing conditions. Staining with Coomassie brilliant blue revealed that these enzymes had been purified to homogeneity (Figure 4). As a final check of correct mutant production and protein purity, all mutants except R30M and Y63A were analyzed by electrospray ionization mass spectroscopy. The measured molecular weights for all recombinant enzymes tested, except F64A and W61A/Y63A/F64A, were within 3 amu of the theoretical value. F64A was 7 amu higher and W61A/Y63A/F64A was 16 amu lower than the respective theoretical values. Western blot analysis of the purified mutants was carried out using a polyclonal antibody raised against native PLA_2. Native, WT,

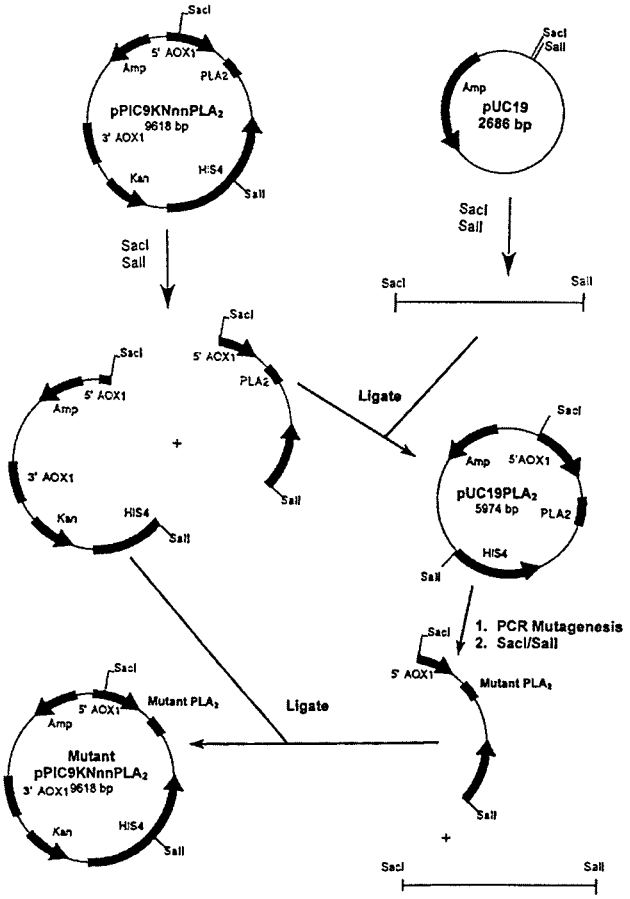

FIGURE 3: Cloning diagram for site-directed mutagenesis. The *P. pastoris* expression vector, pPIC9K*Nnn*PLA_2, and the pUC19 vector were digested with *Sac*I and *Sal*I. The fragment containing the PLA_2 gene and the linearized pUC19 vector were ligated to form pUC19PLA_2. This smaller plasmid was used as the template to construct mutants using a PCR-based methodology. Afterward the mutant PLA_2 gene was transferred back into pPIC9K*Nnn*PLA_2 at the *Sac*I−*Sal*I junction to facilitate expression in yeast.

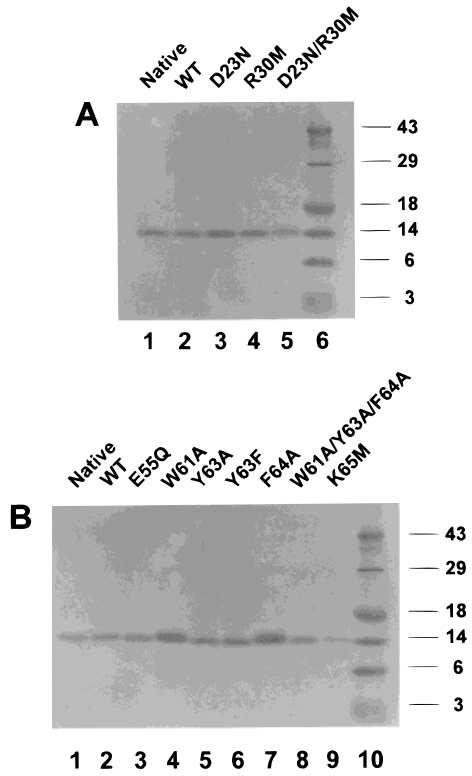

FIGURE 4: SDS−PAGE of WT and mutant PLA_2s. Approximately 3 μg of enzyme was loaded on 18% Tris−glycine gels under denaturing conditions: (A) native (lane 1), WT (lane 2), D23N (lane 3), R30M (lane 4), D23N/R30M (lane 5), and MW standards; (B) native (lane 1), WT (lane 2), E55Q (lane 3), W61A (lane 4), Y63A (lane 5), Y63F (lane 6), F64A (lane 7), W61A/Y63A/F64A (lane 8), K65M (lane 9), and MW standards (lane 10).

and all of the mutants were recognized as a 14 kDa band by the antibody, demonstrating that none of the mutations had affected antibody recognition.

To assess if any gross changes in folding occurred during expression, the CD spectrum of each recombinant enzyme was analyzed. All proteins showed spectra similar to that reported previously for *N. naja naja* PLA_2 with extrema at 208 and 222 nm (*32*), indicating that the expressed mutants contain similar secondary structures and are probably folded correctly.

Monomeric Activity. Rates of hydrolysis for monomeric diC_6-PC were determined using a thin-layer chromatography assay as described in Materials and Methods and are shown in Table 1. Native, WT, and all of the mutants analyzed showed comparable activities on monomeric diC_6-PC. Generally, these enzymes were found to have specific activities between 50 and 80 μmol min^{-1} mg^{-1}, in good agreement with values reported previously (*11*). Such activities demonstrate that the catalytic machinery is intact and provides another line of evidence that the expressed proteins are properly folded.

Headgroup Specificity. To investigate whether any of the mutations altered headgroup specificity, we measured the rates of hydrolysis of binary mixtures of PLPE/PLPC (1:1) in TX-100 mixed micelles under activating conditions. Rates for PE hydrolysis in these micellar binary mixtures were determined by including radiolabeled PLPE in the assay. To determine the rates of PC hydrolysis, separate experiments were run under identical conditions except that radiolabeled PLPC was included in the assay instead of radiolabeled PLPE. As shown in Table 2, native, WT, and the mutants displayed a 4-fold preference for PE headgroups over PC headgroups under these conditions, which is in good agreement with previous reports (*4*−*6*). It should be noted that the Y63A and the W61A/Y63A/F64A mutants had no detectable PC activity. These results indicate that headgroup specificity is not affected by any of the mutations.

Micellar Activity. Rates of hydrolysis on micellar substrates were determined using mixed micelles containing PLPE as shown in Table 3. The D23N, R30M, and D23N/R30M mutants that were constructed to probe the Segelke site displayed near normal activity on micellar PLPE substrates. The nonaromatic E55Q and K65M Ortiz site mutants also showed near normal activity on micellar PLPE substrates. Compared to WT, the aromatic W61A mutant displayed a 3-fold reduced rate of hydrolysis on micellar PLPE substrates and a 2-fold reduced rate of hydrolysis on micellar PLPC substrates. Interestingly, the other aromatic mutants Y63A, Y63F, F64A, and W61A/Y63A/F64A displayed markedly reduced rates, at least 10-fold, of hydrolysis toward micellar PLPE substrates. Since all of these enzymes possessed comparable rates of hydrolysis on monomeric

Table 1: Specific Activities toward Monomeric DiC_6-PC[a]

enzyme	specific activity (μmol min^{-1} mg^{-1})	enzyme	specific activity (μmol min^{-1} mg^{-1})
native	78 ± 14	W61A	113 ± 28
WT	64 ± 9	Y63A	61 ± 18
D23N	67 ± 6	Y63F	64 ± 18
R30M	51 ± 6	F64A	86 ± 21
D23N/R30M	62 ± 4	W61A/Y63A/F64A	51 ± 6
E55Q	97 ± 29	K65M	84 ± 33

[a] DiC_6-PC was utilized at monomeric substrate concentrations well below its critical micelle concentration (CMC) of 14 mM (*28*). Assays contained 0.8 mM diC_6−PC, 25 mM Tris, pH 8.5, and 10 mM $CaCl_2$. Reactions were run at 40 °C for 30 min as described in Materials and Methods. Values are reported as the mean ± standard deviation for triplicate measurements.

Table 2: Headgroup Specificity of Native, WT, and Mutant Enzymes under Activating Conditions[a]

enzyme	PE rate (μmol min^{-1} mg^{-1})	PC rate (μmol min^{-1} mg^{-1})	specificity (fold)
native	752 ± 13	192 ± 5	3.92 ± 0.12
WT	577 ± 12	154 ± 2	3.75 ± 0.09
D23N	29.3 ± 1.80	6.89 ± 0.06	4.25 ± 0.26
R30M	14.8 ± 0.20	3.76 ± 0.13	3.94 ± 0.15
D23N/R30M	25.1 ± 0.6	5.93 ± 0.15	4.23 ± 0.15
E55Q	389 ± 1	106 ± 4	3.67 ± 0.14
W61A	210 ± 3	51.1 ± 2.1	4.11 ± 0.18
Y63A	1.83 ± 0.02	0	N/A[b]
Y63F	31.9 ± 0.8	7.99 ± 0.26	3.99 ± 0.16
F64A	24.0 ± 0.7	6.08 ± 0.31	3.95 ± 0.23
W61A/Y63A/F64A	0.33 ± 0.02	0	N/A[b]
K65M	476 ± 7	116 ± 1	4.10 ± 0.07

[a] Specific activities were determined at 40 °C using a modified Dole assay containing 150 μM PLPE, 150 μM PLPC, 2400 μM Triton X-100, 25 mM Tris, pH 8.5, 100 mM KCl, and 10 mM $CaCl_2$. Radiolabeled PLPE was included to obtain rates of hydrolysis for PE. To determine rates of hydrolysis for PC, separate experiments were run under identical conditions except that only radiolabeled PLPC was included. Values are reported as the mean ± standard deviation for triplicate measurements. [b] N/A, not applicable.

Table 3: Effect of Mutations on Micellar Activity and PC Activation[a]

enzyme	PLPC (μmol min^{-1} mg^{-1})	PLPE (μmol min^{-1} mg^{-1})	PLPE + SPH (μmol min^{-1} mg^{-1})	activation (fold)
native	248 ± 6	10.20 ± 0.50	215 ± 2	21.1 ± 1.1
WT	195 ± 15	7.68 ± 0.35	166 ± 18	21.6 ± 2.5
D23N	3.13 ± 0.78	8.45 ± 0.20	19 ± 1	2.2 ± 0.1
R30M	6.84 ± 0.44	6.64 ± 1.13	76 ± 9	11.5 ± 2.4
D23N/R30M	9.44 ± 0.53	4.30 ± 0.03	12 ± 0.4	2.8 ± 0.1
E55Q	169 ± 4	6.40 ± 0.12	114 ± 3	17.8 ± 0.6
W61A	102 ± 2	2.57 ± 0.05	43 ± 4	16.7 ± 1.6
Y63A	1.22 ± 0.43	0.38 ± 0.03	0.69 ± 0.38	1.8 ± 1.0
Y63F	14.0 ± 0.8	0.71 ± 0.12	9.50 ± 1.12	13.4 ± 2.8
F64A	12.4 ± 1.2	0.26 ± 0.01	6.55 ± 0.34	25.2 ± 1.6
W61A/Y63A/F64A	0.83 ± 0.13	0	0	N/A[b]
K65M	217 ± 5	7.34 ± 0.28	158 ± 2	21.5 ± 0.9

[a] Specific activities for micellar substrates were determined at 40 °C using a modified Dole assay containing 300 μM PLPE or PLPC, 2400 μM Triton X-100, 25 mM Tris, pH 8.5, 100 mM KCl, and 10 mM $CaCl_2$. For activation measurements, 60 μM sphingomyelin was included. Values are reported as the mean ± standard deviation for triplicate measurements. [b] N/A, not applicable.

substrates, the reduced catalytic rates on micellar substrates suggest that these aromatic residues may be important for interfacial activation. These finding are in good agreement with similar studies carried out using porcine pancreatic PLA_2 (*37*) where mutations at position 63 were found to decrease rates of hydrolysis on micellar substrates (*38*).

PC Activation. To assess the effect of the mutations on PC activation, specific activities toward micellar PLPE with and without sphingomyelin were measured using radiolabeled phospholipid. These results are shown in Table 3. In this assay system, native and WT PLA_2 both show a 21-fold activation by sphingomyelin. The E55Q, W61A, Y63F, F64A, and K65M mutants were also activated significantly by sphingomyelin. Of all the mutations to the Ortiz site, only the Y63A mutant shows substantially reduced PC activation. While the rates of hydrolysis with or without sphingomyelin are low, it is clear that Tyr-63 affects PC activation.

Mutations to residues in the Segelke site caused a substantial decrease in PC activation. The D23N mutant decreased activation by 10-fold without substantially affecting the hydrolysis of PLPE alone. Similar results were found with the D23N/R30M mutant where activation is decreased almost 8-fold. Mutations to Arg-30 alone do not appear to affect PC activation nearly as much as Asp-23 mutations since the R30M mutant still shows a nearly 12-fold activation. Thus, mutations to Asp-23 appear to be more critical for PC activation than those to Arg-30. These results support the hypothesis advanced by Segelke et al. (*16*) that the charge

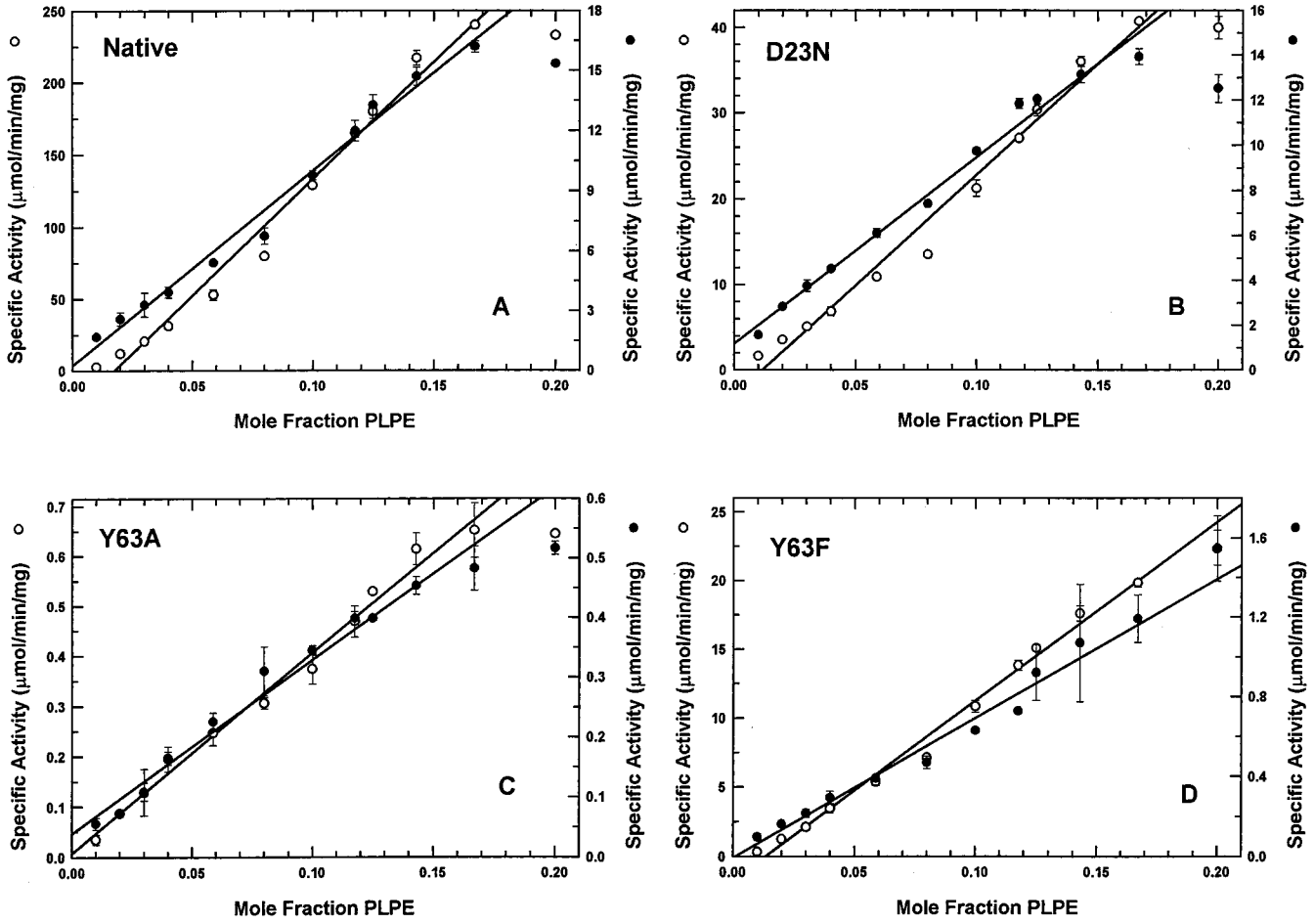

FIGURE 5: Surface dilution kinetics of native and mutant PLA_2s. Plots of specific activity vs mole fraction of PLPE are shown for (A) native, (B) D23N, (C) Y63A, and (D) Y63F PLA_2. In these experiments, the bulk concentration of PLPE was kept constant at 300 μM and its surface concentration varied by the addition of appropriate amounts of TX-100. Assays were carried out at 40 °C and contained 10 mM $CaCl_2$, 25 mM Tris, pH 8.5, and 100 mM KCl. Closed circles are for measurements containing only PLPE as substrate. Open circles represent determinations in the presence of 60 μM sphingomyelin. Data points represent the mean ± standard deviation for duplicate measurements.

on the PC headgroup may be stabilized by Asp-23, with a minor contribution from Arg-30.

Surface Dilution Kinetics. Results of surface dilution experiments are shown in Figure 5. Enzyme activity is clearly dependent upon the surface concentration of the substrate. The axes in Figure 5 are scaled differently to show that the shapes of the curves are essentially unchanged by either mutation or the presence of activator. This implies that the kinetic behavior of these enzymes is similar.

The plots of mole fraction of PLPE versus specific activity for native, D23N, Y63A, and Y63F are all close to linear although there is a subtle break at a mole fraction of 0.07 and a substantial break at a mole fraction of 0.20. The abrupt break at a mole fraction of 0.20 is probably due to the insolubility of the phospholipid in the mixed micelle at high surface phospholipid concentrations. Thus, the enzyme apparently cannot be saturated with substrate due to substrate insolubility. Therefore, the slopes of these curves can only give estimates of the catalytic efficiencies (k_{cat}/K_m). Individual values for k_{cat} and K_m cannot be determined, although it is apparent that the K_m for PLPE is much greater than 0.20 mole fraction.

The apparent catalytic efficiencies were obtained from the slopes of the lines shown in Figure 5. After omitting the 0.20 mole fraction data point, linear regressions for the remaining data points gave a correlation of at least 0.98 for all plots. These results are presented in Table 4. Measurement of the catalytic efficiency with or without activator present was also used to measure activation by sphingomyelin. Direct measurement of activation (shown in Table 3) and kinetic determinations of activation (shown in Table 4) are in good agreement.

Table 4: Activation of Mutant Enzymes[a]

enzyme	k_{cat}/K_m unactivated (s^{-1})	k_{cat}/K_m activated (s^{-1})	activation (fold)
native	22.7	377	16.6
D23N	19.3	60.1	3.1
Y63A	0.676	0.930	1.4
Y63F	1.63	30.3	18.6

[a] Apparent k_{cat}/K_m values were calculated from the slopes of surface dilution kinetic experiments shown in Figure 5. Since K_m is expressed in terms of mole fraction, k_{cat}/K_m is expressed in units of s^{-1}. Due to poor phospholipid solubility in mixed micelles at high lipid surface concentrations, the data point at 0.20 mole fraction was omitted from these calculations. Linear regression for all other mole fractions resulted in a correlation of at least 0.98. Activation values are calculated as the relative increase observed in the presence of sphingomyelin compared to PLPE alone.

DISCUSSION

PC Activation. The minimal requirements for PC activation include a PC headgroup, at least one fatty acyl or alkyl chain, and an interface (*6, 12*). Earlier studies demonstrated that PC activation was due to lipid−protein interactions and could not be accounted for by lipid−lipid interactions in the micelles (*5*). These observations led to the postulation of a two-site model where the enzyme contains both a catalytic site with a preference for zwitterionic phospholipids and a separate activator site that is specific for PC-containing compounds. To test this model, we utilized site-directed mutagenesis to determine where the PC activator site is located on cobra PLA_2. Thus far, two regions of the enzyme have been identified as possible PC activator sites.

Ortiz Site. The first location proposed for the PC activator site was based on the molecular modeling studies of Ortiz et al. (*15*) and consisted of residues Glu-55, Trp-61, Tyr-63, Phe-64, and Lys-65, which are located in the elapid loop of the enzyme. Enzymes containing mutations designed to disrupt these proposed aromatic interactions displayed rates of hydrolysis toward monomeric diC_6-PC substrates that were similar to those of native and WT PLA_2. Apparently, this region of the molecule is not critical for monomeric activity. These results also imply that the mutants possessed functional catalytic sites and were properly folded. The W61A, Y63A, Y63F, F64A, and W61A/Y63A/F64A mutants all displayed reduced rates of hydrolysis toward micellar PLPE substrates. Under these conditions, i.e., without PC, PC activation is not possible, therefore this reduction in rate is presumably due to a decrease in interfacial activation and not PC activation. The latter observation was confirmed when sphingomyelin was included. With activator present, all of the mutants except Y63A exhibited full PC activation. These results suggest that the aromatic amino acids of the elapid loop are important for interfacial activation but not for basal catalysis, headgroup specificity, or PC activation.

Role of Tyrosine-63. The Y63A mutant was the only exception to the general trends mentioned above in that it affected both interfacial and PC activations. Previous studies with porcine pancreatic PLA_2 have shown that mutagenesis of Tyr-69 (Tyr-63 of *N. naja naja* PLA_2 and Tyr-69 of porcine pancreatic PLA_2 are equivalent) significantly reduces enzyme activity on micellar substrates and also causes a loss of substrate stereospecificity (*37, 38*). Crystallographic studies have elucidated two important roles for Tyr-69. In the crystal structure of *Naja naja atra* PLA_2 with a bound inhibitor (*39*), the Tyr-69 forms a hydrogen bond with the *sn*-3 phosphate oxygen of the substrate and also serves as a hydrophobic flap that keeps the substrate productively bound in the active site. Crystal structures of *N. naja naja* PLA_2 complexed with an inhibitor are not available, but examination of the various uninhibited subunits found in three different *N. naja naja* PLA_2 crystal forms reveals that the Tyr-63 side chain adopts several conformations. These observations suggest that the Tyr-63 side chain in the *N. naja naja* PLA_2 can also function as a moveable hydrophobic flap.

The Y63A mutant abolishes both the hydrogen-bonding ability of Tyr-63 and its ability to function as a hydrophobic flap while the Y63F mutant only prevents hydrogen bond formation without appreciably affecting the hydrophobicity of the side chain at this position. Surprisingly, both the Y63A and Y63F mutants display similar rates of hydrolysis toward monomeric diC_6-PC substrates when compared to native and WT PLA_2. These results imply that the formation of a hydrogen bond between Tyr-63 and the *sn*-3 phosphate oxygen of the substrate is not important for the hydrolysis of monomeric substrates in *N. naja naja* PLA_2. However, rates of hydrolysis on micellar PLPE substrates are drastically reduced for both the Y63A and Y63F mutants. This suggests that the hydrogen-bonding ability of Tyr-63 may be important for interfacial activation. With regard to PC activation, the Y63A mutant shows little if any PC activation, while the Y63F mutant is still activated 13-fold by sphingomyelin. This suggests that the hydrophobicity of residue 63 is important for PC activation. To summarize, Tyr-63 is not directly involved in the catalysis of monomeric substrates; however, its hydroxyl group and presumably its ability to form a hydrogen bond are critical for interfacial catalysis, and its hydrophobicity is important for PC activation.

Role of Tryptophan-61. Recent mutagenesis experiments with bovine pancreatic PLA_2 (*40*) and human group IIA PLA_2 (*41*) have reported that tryptophan residues on these enzymes may be important for binding PC interfaces. Tryptophan residues have also been shown to facilitate membrane penetration via insertion of the aromatic ring into the lipid interface (*42*). The PLA_2 isoforms from the sea snake *Laticauda semifasciata* that lack tryptophan residues have an impaired ability to hydrolyze micellar PC substrates (*43*). *N. naja naja* PLA_2 contains three tryptophans at positions 18, 19, and 61. Our findings demonstrate that the W61A mutant does not affect monomeric activity, PE versus PC headgroup specificity, or PC activation; however, rates of hydrolysis on both micellar PLPC and PLPE substrates are reduced by about 50%. Thus, Trp-61 in the *N. naja naja* PLA_2 does not appear to play the same dramatic role that is seen for tryptophan in other PLA_2s.

Segelke Site. A second possible location for the PC activator site (*16*) was a region near residues Asp-23 and Arg-30 that has good electrostatic and shape complementarity to a PC headgroup. The D23N, R30M, and D23N/R30M mutants were designed to disrupt these interactions. The rates of hydrolysis on monomeric diC_6-PC substrate were similar to those of native and WT PLA_2, demonstrating that these mutants have normal monomeric activity. These results also imply that the mutants possessed fully functional catalytic sites and were probably folded correctly. Rates of hydrolysis on micellar PLPE alone showed only modest changes compared to those of native and WT, suggesting that these residues are not involved in interfacial activation. However, measurements of micellar PLPE hydrolysis in the presence of sphingomyelin revealed that PC activation was decreased by nearly 10-fold for both the D23N and D23N/R30M mutants. The R30M mutant was still activated nearly 12-fold by sphingomyelin. These results suggest that the negatively charged Asp-23 side chain is critical for PC activation and that the reduced rates of hydrolysis of the D23N mutant on micellar PLPC substrates (Table 3) are probably due at least in part to the lack of PC activation.

Interfacial Activation and PC Activation. The cobra venom PLA_2 is unique among the PLA_2s in that it exhibits both PC and interfacial activations. Because of the nature of these two activations, it has been difficult to determine whether they are separate, distinct phenomena or represent different

facets of the same process. The mutagenesis studies reported here have shed some light on this question. We have shown that mutating the aromatic residues in the Ortiz site significantly reduced interfacial activation while mutations to the Segelke site did not. Conversely, mutations to the Segelke site affected PC activation but not interfacial activation. Thus, it is possible to independently disrupt these activations. This strongly suggests that these are two separate processes. Almost all of the evidence presented here is consistent with this hypothesis except for the Y63A mutant, which is the only Ortiz site mutant that significantly reduced PC activation.

Why is the Y63A mutant the only one to affect both activations? A possible explanation is suggested in Figures 1 and 2. The Ortiz site residues are far enough removed from the Segelke residues to preclude any direct interaction between the two sites. The one exception again is Tyr-63. Its aromatic ring, which forms the hydrophobic flap, is in the vicinity of and oriented toward the Arg-30 side chain. Because there are no crystal structures with a PC molecule bound to the enzyme other than in the catalytic site, we have no information about the orientation of Tyr-63 when a PC activator is bound in the Segelke site. It appears that the Arg-30 side chain should be fairly flexible and may in fact orient in such a way that it does interact with the Tyr-63 or that it interacts with the substrate close to where Tyr 63 does. Such an interaction may affect the ability of Tyr-63 to function as the hydrophobic flap. Thus, it is likely that these are two independent activations that involve the same region of the enzyme and its interactions with substrate.

In general, the two most often proposed mechanisms for either PC activation or interfacial activation are an enzyme conformational change or a substrate concentration effect. Both of these mechanisms are consistent with the results reported here. The binding of the PC in the Segelke site could alter the orientation of Arg-30 in such a way as to change its interaction with the substrate or to alter the functioning of the Tyr-63 hydrophobic flap. Binding of PC to the Segelke site could also sequester the enzyme to the surface. This would increase the amount of time that the enzyme remains on the surface, permitting greater processivity. Similar arguments can be applied to the binding of phospholipids in the Ortiz site to explain interfacial activation.

A third possible mechanism of activation involves the orientation of the enzyme with respect to the interface and the phospholipids in it. As shown in Figures 1 and 2, the face of the enzyme that contains the active site cleft is rather large, and there may be any number of points of attachment between the enzyme and the surface. We have identified three, the Ortiz, the Segelke, and the catalytic sites. The presence of three PL binding sites raises the possibility that these sites hold the enzyme in a particular orientation with respect to both the interface and the individual molecules in it and that this orientation offers the lowest energy route for the substrate to reach the catalytic site. All of these sites may also be required to hold the enzyme in a position to maintain the desolvation of the area between the enzyme and the interface. The desolvation of this region has been proposed as an important contributor to interfacial activation (*44*). Any change in the attachments could affect this desolvation.

In the end, all three effects probably contribute to these activations. For example, one possible scenario that would explain our data is that PC activation requires a conformational change that occurs only when the PC is bound to the Segelke site and interfacial activation is due to enzyme orientation and/or desolvation, which requires that all three attachment sites be occupied. If mutations to Asp-23 prevent the conformational change required for PC activation but do not prevent the binding of PC, then PC activation would be disrupted but the interfacial activation would still be intact because the Segelke site would have a PC bound and all three attachments would still be in effect and the enzyme would be correctly oriented. If, on the other hand, the Ortiz site is mutated and no longer binds phospholipid correctly, one of the anchors would be lost and the enzyme could reorient, causing the loss of interfacial activation. PC could still bind to the Segelke site and cause the correct enzyme conformational change, and thus, PC activation would be preserved. Certainly, other scenarios should also be considered.

Conclusion. These results represent the first use of the *P. pastoris* yeast expression system to produce milligram quantities of an $sPLA_2$ without the need for in vitro refolding. They also constitute the first experimental evidence that identifies a PC activator site, the Segelke site, in *N. naja naja* PLA_2 and indicates a possible location for an interfacial recognition site, the Ortiz site. These studies also indicate that interfacial and PC activation are not one in the same process since they are differentially affected by these mutations.

ACKNOWLEDGMENT

The authors are extremely grateful to Professor Elizabeth A. Komives and Dr. Christopher E. White for excellent guidance with the *P. pastoris* gene expression system and for first suggesting its use, Mark Pandori for assistance with vector construction, Matt Williamson of the UCSD Biology Department Protein Sequencing Facility for N-terminal sequencing, Larry A. Gross of the Howard Hughes Medical Institute for electrospray ionization mass spectroscopy, and Joseph Taulane and Kerri M. Zawadzki for assistance with circular dichroism measurements. The authors also thank Dr. Scott C. Boegeman and Dr. Brent W. Segelke for critical discussions.

REFERENCES

1. Dennis, E. A. (1994) *J. Biol. Chem. 269*, 13057.
2. Dennis, E. A. (1997) *Trends Biochem. Sci. 22*, 1.
3. Balsinde, J., Balboa, M. A., Insel, P. A., and Dennis, E. A. (1999) *Annu. Rev. Pharmacol. Toxicol. 39*, 175.
4. Adamich, M., and Dennis, E. A. (1978) *Biochem. Biophys. Res. Commun. 80*, 424.
5. Roberts, M. F., Adamich, M., Robson, R. J., and Dennis, E. A. (1979) *Biochemistry 18*, 3301.
6. Adamich, M., Roberts, M. F., and Dennis, E. A. (1979) *Biochemistry 18*, 3308.
7. Pluckthun, A., and Dennis, E. A. (1982) *Biochemistry 21*, 1750.
8. Hendrickson, H. S., and Dennis, E. A. (1984) *J. Biol. Chem. 259*, 5740.
9. Yu, L., and Dennis, E. A. (1993) *Biochemistry 32*, 10185.
10. Pluckthun, A., Rohlfs, R., Davidson, F. F., and Dennis, E. A. (1985) *Biochemistry 24*, 4201.
11. Lombardo, D., and Dennis, E. A. (12−25−1985) *J. Biol. Chem. 260*, 16114.

12. Dennis, E. A., and Pluckthun, A. (1986) in *Enzymes of Lipid Metabolism II* (Freysz, L., Dreyfus, A., Massarelli, R., and Gatt, S., Eds.) pp 121−131, Plenum, New York.
13. Roberts, M. F., Deems, R. A., and Dennis, E. A. (1977) *Proc. Natl. Acad. Sci. U.S.A. 74*, 1950.
14. Hazlett, T. L., Deems, R. A., and Dennis, E. A. (1990) *Adv. Exp. Med. Biol. 279*, 49.
15. Ortiz, A. R., Pisabarro, M. T., Gallego, J., and Gago, F. (1992) *Biochemistry 31*, 2887.
16. Segelke, B. W., Nguyen, D., Chee, R., Xuong, N. H., and Dennis, E. A. (1998) *J. Mol. Biol. 279*, 223.
17. Kelley, M. J., Crowl, R. M., and Dennis, E. A. (1992) *Biochim. Biophys. Acta 1118*, 107.
18. Bianco, I. D., Kelley, M. J., Crowl, R. M., and Dennis, E. A. (1995) *Biochim. Biophys. Acta 1250*, 197.
19. Sanger, F., Nicklen, S., and Coulson, A. R. (1977) *Proc. Natl. Acad. Sci. U.S.A. 74*, 5463.
20. White, C. E., Kempi, N. M., and Komives, E. A. (1994) *Structure 2*, 1003.
21. White, C. E., Hunter, M. J., Meininger, D. P., White, L. R., and Komives, E. A. (1995) *Protein Eng. 8*, 1177.
22. Chen, Y., Cino, J., Hart, G., Freedman, D., White, C. E., and Komives, E. A. (1997) *Process Biochem. 32*, 107.
23. Hazlett, T. L., and Dennis, E. A. (1985) *Toxicon 23*, 457.
24. Lowry, O. H., Rosebrough, N. J., Farr, A. L., and Randall, R. J. (1951) *J. Biol. Chem. 193*, 265.
25. Darke, P. L., Jarvis, A. A., Deems, R. A., and Dennis, E. A. (1980) *Biochim. Biophys. Acta 626*, 154.
26. Yu, L., and Dennis, E. A. (1991) *Methods Enzymol. 197*, 65.
27. Adamich, M., and Dennis, E. A. (1978) *J. Biol. Chem. 253*, 5121.
28. Lio, Y. C., and Dennis, E. A. (1998) *Biochim. Biophys. Acta Lipids Lipid Metab. 1392*, 320.
29. Turner, J. D., and Rouser, G. (1970) *Anal. Biochem. 38*, 423.
30. Bartlett, G. R. (1959) *J. Biol. Chem. 234*, 466.
31. Conde-Frieboes, K., Reynolds, L. J., Lio, Y., Hale, M., Wasserman, H. H., and Dennis, E. A. (1996) *J. Am. Chem. Soc. 118*, 5519.
32. Davidson, F. F., and Dennis, E. A. (1990) *Biochim. Biophys. Acta 1037*, 7.
33. Dougherty, D. A. (1996) *Science 271*, 163.
34. Cregg, J. M., Vedvick, T. S., and Raschke, W. C. (1993) *Bio/Technology 11*, 905.
35. Scott, D. L., and Sigler, P. B. (1994) *Adv. Protein Chem. 45*, 53.
36. Orr, J. W., Keranen, L. M., and Newton, A. C. (1992) *J. Biol. Chem. 267*, 15263.
37. Kuipers, O. P., Dijkman, R., Pals, C. E., Verheij, H. M., and De Haas, G. H. (1989) *Protein Eng. 2*, 467.
38. Kuipers, O. P., Dekker, N., Verheij, H. M., and De Haas, G. H. (1990) *Biochemistry 29*, 6094.
39. White, S. P., Scott, D. L., Otwinowski, Z., Gelb, M. H., and Sigler, P. B. (1990) *Science 250*, 1560.
40. Lee, B. I., Yoon, E. T., and Cho, W. H. (1996) *Biochemistry 35*, 4231.
41. Baker, S. F., Othman, R., and Wilton, D. C. (1998) *Biochemistry 37*, 13203.
42. Jacobs, R. E., and White, S. H. (1989) *Biochemistry 28*, 3421.
43. Yoshida, H., Kudo, T., Shinkai, W., and Tamiya, N. (1979) *J. Biochem. (Tokyo) 85*, 379.
44. Gelb, M. H., Jain, M. K., Hanel, A. M., and Berg, O. G. (1995) *Annu. Rev. Biochem. 64*, 653.
45. Plesniak, L. A., Boegeman, S. C., Segelke, B. W., and Dennis, E. A. (1993) *Biochemistry 32*, 5009.
46. Nicholls, A., Sharp, K. A., and Honig, B. (1991) *Proteins 11*, 281.

BI991432T